Inorganica Chimica Acta, *173* (1990) 181–190

Binuclear Manganese(II) and Nickel(II) Complexes with a Potentially Octadentate Macrocyclic Ligand (H_4L1): Synthesis and Characterisation. X-ray Crystal Structures of $[Mn_2(H_2L1)(CH_3COO)_2]\cdot 2CH_3OH$ and $[Ni_2(H_2L1)(H_2O)_2Cl_2]\cdot 2H_2O$

ALISON J. DOWNARD, VICKIE MCKEE* and SANTOKH S. TANDON

Department of Chemistry, University of Canterbury, Christchurch (New Zealand)

(Received January 12, 1990)

Abstract

A series of binuclear manganese(II) and nickel(II) complexes of the macrocyclic ligand H_4L1 has been prepared and characterised. ($[Mn_2(H_2L1)A_2]$, where A = Cl^-, Br^-, NO_3^-, NCS^-, CH_3COO^- or N_3^-; $[Ni_2(H_2L1)X_2Y_2]$, where X = Cl^-, Br^- or NO_3^- and Y = H_2O, $[Ni_2(H_2L1)(NCS)_2(C_2H_5OH)]$ and $[Ni_2(H_2L1)(CH_3COO)_2]\cdot 2H_2O$).

The macrocycle is formed by Schiff base condensation of two molecules of 2,6-diformyl-4-methylphenol with two molecules of 1,3-diamino-2-hydroxypropane in the presence of Ni(II) or Mn(II) as template ion. The complexes are all binuclear with the two metal ions bridged by the deprotonated phenolate donors of the macrocycle. The alcohol groups of the macrocyclic ligand do not coordinate to the metal ions. The complexes have been characterised by analytical, spectroscopic, electrochemical and magnetic susceptibility measurements and the single crystal X-ray structures of $[Mn_2(H_2L1)(CH_3COO)_2]\cdot 2CH_3OH$ (triclinic, $P\bar{1}$, a = 8.701, b = 10.258, c = 10.612 Å, α = 62.44, β = 67.83, γ = 77.74°, V = 776.8 Å^3, Z = 1) and of $[Ni_2(H_2L1)(H_2O)_2Cl_2]\cdot 2H_2O$ (rhombohedral, $R\bar{3}$, a = 28.885, c = 9.783 Å, V = 7069 Å^3, Z = 9) have been determined.

Introduction

Synthetic model studies involving magnetically coupled bi- and polynuclear transition metal systems have attracted much current interest. This is in large measure due to the expectation that such studies will provide deeper insights into complex biological processes. Many metalloenzymes catalyse important reactions at coupled metal centres. The chemistry of manganese has recently come under intense study because of the involvement of manganese ions in the oxygen evolving complex (OEC) of photosystem II [1] and in the pseudocatalase enzyme in *Lactobacillus planatrum* [2]. It is thought that the active site of the OEC involves four manganese centres while that of pseudocatalase is apparently binuclear, however neither the structures of the active sites nor the mechanisms of the water oxidation and peroxide disproportionation reactions are yet understood. A number of nickel-containing enzymes are also known [3]. These systems are poorly understood, although interest in them is increasing. Jack bean urease has been shown to contain two nickel atoms per protein unit. EXAFS studies [4] suggest that the nickel atoms have octahedral geometry and are bonded to nitrogen donors, probably of histidine groups. As the basic biochemistry of these systems becomes established, synthetic modelling studies are becoming feasible [5].

A number of recent papers describe binuclear manganese systems in various oxidation states. In a number of cases the complexes have self-assembled in the presence of mononucleating and bridging ligands [6–8]. In other examples macrocyclic ligands have been used to maintain the manganese centres in close proximity [9, 10]; these sometimes contain potentially bridging groups to provide a pathway for antiferromagnetic coupling. Recently, we reported the preparation and structure of a tetranuclear, mixed-valence $Mn_2^{II}Mn_2^{III}$ complex of the macrocyclic ligand H_4L4 [11]. In this complex the two valence states were clearly distinguishable but antiferromagnetic coupling was present, mediated by alkoxy, phenoxy, oxo and carboxylate bridges. Tuchagues *et al.* have reported bi- and polynuclear manganese complexes formed with the Schiff base macrocyclic ligands H_2L2 and H_3L3 [12]. In a recent paper we reported the preparation, properties and X-ray crystal structures of Pb(II) and Ba(II) complexes with H_4L1 [13]. In this paper we extend this study to include the synthesis and properties of some binuclear manganese(II) and nickel(II) complexes of this ligand.

---

*Author to whom correspondence should be addressed.

0020-1693/90/$3.50

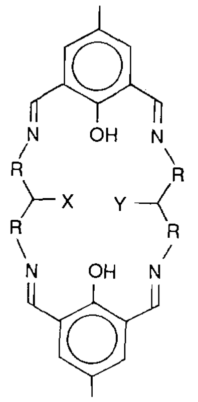

H_4L1 R = CH_2 , X = Y = OH

H_2L2 R = CH_2 , X = Y = H

H_3L3 R = CH_2 , X = H, Y = OH

H_4L4 R = $(CH_2)_2$, X = Y = OH

Experimental

Materials

The solvents were dried by standard procedures. 2,6-Diformyl-4methylphenol was synthesised by the literature procedure. 1,3-Diamino-2-hydroxypropane was used as supplied by Aldrich. All other chemicals used were analar or reagent grade and were used without further purification.

Physical Measurements

IR spectra of the solid samples were recorded as KBr discs on a Pye Unicam SP3-300 infrared spectrc photometer. Electronic spectra were recorded in DMF solution on a Varian DMS100 UV–Vis spectrophotometer in the range 200–850 nm. Magnetic measurements were carried out by the Gouy method from room temperature to liquid nitrogen temperature. The apparatus was supplied by Newport Instruments. The tube was calibrated with $[Ni(en)_3]S_2O_3$. Electrochemical data were obtained using a PAR model 273 potentiostat/galvanostat and a model 175 universal programmer. A single compartment cell containing a glassy carbon disc working electrode (area = 0.07 cm^2), a Pt wire auxiliary electrode and a silver wire pseudo-reference electrode was used and *in situ* ferrocene (Fc) enabled the measured potentials to be referenced to the SCE. Unless otherwise stated, all cyclic voltammograms were recorded at room temperature at a scan rate of 100 mV s^{-1} in DMF/0.1 M tetraethylammonium perchlorate (TEAP) using 1 mM complex. In this electrolyte $E^{\circ\prime}$ (Fc^+/Fc) = 0.3 V versus SCE. C, H and N analysis were carried out by the Microanalytical Unit at Otago University, Dunedin. Metals were determined volumetrically using EDTA titration.

Synthesis of the Complexes

$[Mn_2(H_2L1)Cl_2]\cdot H_2O$ (1)

Manganese(II) chloride (2 mmol) and 2,6-diformyl-4-methylphenol (2 mmol) were dissolved in 30 ml of boiling methanol to give a yellow solution which was refluxed for *c.* 10 min. To this, a solution of 1,3-diamino-2-hydroxypropane (2 mmol), dissolved in 20 ml of methanol was added dropwise with constant shaking. A yellow precipitate separated from a reddish brown solution. It was stirred at ambient temperature for *c.* 30 min and kept at r.t. overnight. The yellow solid was filtered, washed with methanol (3 X 10 ml) and dried *in vacuo* overnight (yield 50%). *Anal.* Calc. for $C_{24}H_{28}N_4O_5Cl_2Mn_2$: C, 45.49; H, 4.42; N, 8.85; Mn, 17.37. Found: C, 45.71; H, 4.66; N, 8.80; Mn, 16.89%.

$[Mn_2(H_2L1)Br_2]$ (2)

Manganese(II) bromide (2 mmol) was dissolved in 30 ml of ethanol. To it was added 2,6-diformyl-4-methylphenol (2 mmol) dissolved in 20 ml of ethanol and the yellow solution formed was refluxed for *c.* 15 min. To the boiling reaction mixture, a solution of 1,3-diamino-2-hydroxypropane (2 mmol) in 10 ml of ethanol was added dropwise with shaking. After the addition a yellow solid separated, it was filtered immediately from the hot solution and washed with hot ethanol (3 X 10 ml). It was dried *in vacuo* at r.t. for 24 h (yield *c.* 40%). *Anal.* Calc. for $C_{24}H_{26}N_4O_4Br_2Mn_2$: C, 40.91; H, 3.69; Mn, 15.63. Found: C, 41.04; H, 4.21, Mn, 15.33%.

$[Mn_2(H_2L1)(NO_3)_2]$ (3)

To a solution of manganese(II) nitrate (2 mmol) in ethanol (20 ml) was added a solution of 2,6-diformyl-4-methyl-phenol (2 mmol) in 15 ml of ethanol and the yellow solution thus formed was refluxed for *c.* 10 min and allowed to cool to ambient temperature. To this a solution of 1,3-diamino-2-hydroxypropane (2 mmol) in ethanol (10 ml) was added dropwise, with stirring at r.t. It was further stirred at r.t. for 15 min and the yellow solid which separated from the reddish brown solution was filtered, washed with ethanol (3 X 10 ml) and dried *in vacuo* for 24 h (yield *c.* 40%). *Anal.* Calc. for $C_{24}H_{26}N_6O_{10}Mn_2$: C, 43.11; H, 3.89; N, 12.57; Mn, 16.47. Found: C, 43.27; H, 4.17; N, 12.19; Mn, 16.22%.

$[Mn_2(H_2L1)(NCS)_2]$ (4)

This compound was synthesised in the same manner as described for $[Mn_2(H_2L1)(NO_3)_2]$, but using $Mn(NCS)_2$ (yield *c.* 50%). *Anal.* Calc. for $C_{26}H_{26}N_6O_4Mn_2$: C, 47.27; H, 3.92; Mn, 16.67. Found: C, 47.48; H, 4.42; Mn, 16.32%.

$[Mn_2(H_2L1)(CH_3COO)_2]\cdot 2CH_3OH$ (5)

To a solution of $[Mn(CH_3COO)_2]\cdot 4H_2O$ (2 mmol) in DMF (15 ml) was added 2,6-diformyl-4-methylphenol (2 mmol) dissolved in hot methanol (25 ml). A yellow solution formed, was refluxed for *c.* 15 min and to it, while refluxing and stirring, was added a solution of 1,3-diamino-2-hydroxy-propane (2 mmol) in methanol (10 ml); the reaction mixture acquired a reddish brown colour. It was stirred at r.t. for 40 h, then concentrated on a rotary evaporator to *c.* 20 ml and filtered. The filtrate, while hot, was treated with ether dropwise until some turbidity was apparent in the dark brown solution. It was left a r.t. and after two days, golden yellow crystals separated from the solution. These were filtered, washed with methanol (3 X 3 ml) and dried *in vacuo* for 24 h (yield *c.* 40%). *Anal.* Calc. for $C_{27}H_{34}N_4O_9Mn_2$: Mn, 15.85. Found: Mn 15.22%.

$[Mn_2(H_2L1)(N_3)_2]$ (6)

$[Mn_2(H_2L1)(CH_3COO)_2]\cdot 2CH_3OH$ (1 mmol) was dissolved in boiling methanol (200 ml). To this refluxing solution sodium azide (2 mmol) in hot methanol (40 ml) was added dropwise with constant stirring. The reaction mixture was refluxed for *c.* 10 min and left at ambient temperature. After two days, golden yellow crystals separated from the brown solution. These were filtered and washed with methanol (3 X 10 ml), then dried *in vacuo* at 60 °C for 12 h (yield 80%). *Anal.* Calc. for $C_{24}H_{26}N_{10}O_4Mn_2$: C, 45.86; H, 4.14; N, 22.29; Mn, 17.52. Found: C, 45.85; H, 4.19; N, 21.48; Mn, 17.28%.

$[Ni_2(H_2L1)(H_2O)_2Cl_2]\cdot 2H_2O$ (7)

To a solution of nickel(II) chloride hexahydrate (2 mmol) in methanol, (20 ml), was added a solution of 2,6-diformyl-4-methylphenol (2 mmol) in hot methanol (15 ml) and the pale green solution obtained, was refluxed for *c.* 15 min. While refluxing, 1,3-diamino-2-hydroxypropane (2 mmol) dissolved in methanol (10 ml) was added dropwise over 10–15 min and the dark green solution which formed was refluxed for *c.* 20 h. This was concentrated on a rotary evaporator to *c.* 20 ml, when a green crystalline complex separated from a yellowish green solution. It was filtered, washed with ethanol (3 X 10 ml) and dried *in vacuo* at *c.* 60 °C for 8 h (yield 72%). *Anal.* Calc. for $C_{24}H_{30}N_4O_6Cl_2Ni_2$: C, 43.74; H, 4.56; Ni, 17.83. Found: C, 43.81; H, 5.01; Ni, 17.59%.

$[Ni_2(H_2L1)(H_2O)_2[Br_2]\cdot 2H_2O$ (8)

Nickel(II) bromide hexahydrate (2 mmol) and 2,6-diformyl-4-methylphenol (2 mmol) were dissolved in dry, boiling ethanol (40 ml) and the yellowish green solution thus formed was refluxed for *c.* 15 min. While refluxing, a solution of 1,3-diamino-2-hydroxypropane (2 mmol) in dry ethanol (10 ml) was added dropwise with frequent shaking. A yellowish green solid separated immediately; it was filtered hot, washed with dry ethanol (3 X 10 ml) and dried *in vacuo* at 60 °C for 8 h (yield 71%). *Anal.* Calc. for $C_{24}H_{34}N_4O_8Br_2Ni_2$: C, 36.76; H, 5.36; Ni, 14.99. Found: C, 37.01; H, 4.74; Ni, 14.31%.

$[Ni_2(H_2L1)(H_2O)_2(NO_3)_2]\cdot H_2O$ (9)

To a refluxing mixture of nickel(II) nitrate hexahydrate (2 mmol) and 2,6-diformyl-4-methylphenol (2 mmol) in dry ethanol (50 ml) a solution of 1,3-diamino-2-hydroxypropane in dry ethanol (10 ml) was added dropwise with frequent shaking. At first, a bright green solution formed which, after refluxing for *c.* 1 h, changed into yellowish green. It was further refluxed for *c.* 20 h and was concentrated to *c.* 10 ml on a rotary evaporator and left overnight at ambient temperature. A green solid separated which was filtered, washed with dry ethanol (3 X 10 ml) and dried *in vacuo* at 60 °C for 8 h (yield 55%). *Anal.* Calc. for $C_{24}H_{32}N_6O_{13}Ni_2$: C, 39.48; H, 4.39; Ni, 16.09. Found: C, 39.87; H, 4.74; Ni, 15.83%.

$[Ni_2(H_2L1)(NCS)_2C_2H_5OH]$ (10)

Nickel(II) thiocyanate was prepared by reacting quantitative amounts of nickel(II) nitrate hexahydrate and potassium thiocyanate in a mixture of dry methanol: dry ethanol (1:1, 30 ml). To the above solution of nickel(II) thiocyanate (2 mmol), was added a solution of 2,6-diformyl-4-methylphenol (2 mmol) in dry ethanol (20 ml) and the reaction mixture was refluxed for *c.* 10 min. To this refluxing solution a solution of 1,3-diamino-2-hydroxy-propane (2 mmol) in dry ethanol (10 ml) was added, dropwise with shaking, and a colour change from bright green to greenish brown and finally to dull green took place. After refluxing for *c.* 20 m, dull green solid started separating from the yellowish brown solution. It was further refluxed for 1 h, filtered hot, washed with dry hot ethanol (3 X 10 ml) and dried *in vacuo* at 60 °C for 8 h (yield 67%). *Anal.* Calc. for $C_{28}H_{32}N_6O_6S_2Ni_2$: C, 47.10; H, 4.49; Ni, 16.45. Found: C, 47.37; H, 4.66; Ni, 16.11%.

$[Ni_2(H_2L1)(CH_3COO)_2]\cdot 2H_2O$ (11)

This complex was isolated by the same method as described for $[Ni_2(H_2L)(H_2O)_2(NO_3)_2]\cdot H_2O$, but using nickel(II) acetate tetrahydrate. In this case, the reaction mixture, after refluxing for *c.* 20 h was concentrated to *c.* 5 ml on a rotary evaporator and the yellowish green complex was separated by adding petroleum ether in excess. It was filtered and dissolved in dichloromethane (30 ml). Some insoluble solid was filtered off and the filtrate was concentrated to dryness on a rotary evaporator and dried *in vacuo* at 60 °C for 8 h (yield 78%). *Anal.* Calc. for $C_{28}H_{36}N_4O_{10}Ni_2$: C, 47.63; H, 5.10; Ni, 16.64. Found: C, 47.27; H, 5.32; Ni, 16.39%.

Crystallography

Crystal data for 5

$C_{30}H_{40}N_{10}O_9Mn_2$, crystal dimensions 0.6 × 0.2 × 0.16 mm, triclinic, $a = 8.701(2)$, $b = 10.258(3)$, $c = 10.612(2)$ Å, $\alpha = 62.44(2)$, $\beta = 67.83(2)$, $\gamma = 77.74(2)^\circ$, $V = 776.8(3)$ Å^3, space group $P\bar{1}$, $Z = 1$, $F(000) = 392$. 2° ω-scans at 4.88° min^{-1} were used to collect 2730 unique reflections in the range $4 < 2\theta < 50^\circ$, and 2402 with $I > 2\sigma(I)$ were used in the refinement.

Crystal data for 7

$C_{24}H_{34}N_4O_8Cl_2Ni_2$, crystal dimensions, 0.48 × 0.46 × 0.20 mm, rhombohedral, $a = 28.885(4)$, $c = 9.783(3)$ Å, $V = 7069(3)$ Å^3, space group $R\bar{3}$, $Z = 9$, $F(000) = 3221$. 1.6° ω-scans at 5.3° min^{-1} were used to collect 2059 unique reflections in the range $4 < 2\theta < 45^\circ$, and 1521 with $I > 3\sigma(I)$ were used in the refinement.

Both data sets were collected at 160 K on a Nicolet R3M four-circle diffractometer using graphite-monochromated Mo Kα radiation. Crystal stabilities were monitored by recording three check reflections every 100 reflections and no significant variations were observed. The data sets were corrected for Lorentz and polarisation effects and empirical absorption corrections were applied. The structures of both compounds **5** and **7** were solved from Patterson calculations which revealed the positions of the metal atoms and the structures were developed from difference Fourier calculations. In each case all non-hydrogen atoms were refined with anisotropic temperature factors and the hydrogen atoms were inserted at calculated positions using a riding model with thermal parameters set to 1.2 U of the carrier atom. The refinement of **5** converged with $R = 0.0407$ and $R_w = 0.0568$, for **7**, the corresponding values were $R = 0.073$, $R_w = 0.114$. The structures were refined by blocked cascade least-squares techniques. The function minimised in the refinement was $\Sigma w(|F_o| - |F_c|)^2$ where $w = [\sigma^2(F_o) + gF_o{}^2]^{-1}$ and $g = 0.000327$ and 0.0045, respectively. All programs used for data collection and structure solution are contained in the SHELXTL (version 4.1) package [14].

Results and Discussion

Synthesis

Condensation of one equivalent each of 2,6-diformyl-4-methylphenol (dfmp) and 1,3-diamino-2-hydroxypropane (dahp) in the presence of Mn(II) or Ni(II) template ions yielded binuclear complexes of the macrocycle H_4L1. The phenolic groups of the macrocycle are deprotonated and bridge the two metal ions. The alcohol groups retain their protons and are not involved in coordination to the metal ions.

Only binuclear products have been obtained, even when a metal ligand ratio of 4:1 is used. This contrasts with the behaviour of the larger macrocycle H_4L4 which can bind four metal ions utilising both alkoxy and phenoxy groups as endogenous bridges. The difference between the two ligands can be ascribed to the relative sizes of their macrocyclic cavities. More precisely, the saturated chains in H_4L1 are too short to accommodate the alcohol groups in the plane of the phenoldiimine groups.

A series of eleven binuclear manganese(II) and nickel(II) complexes has been prepared and characterised (Table 1). Complexes **5** and **7** have been investigated by X-ray crystallography, the formulae of the remaining complexes were deduced from microanalytical and spectroscopic data. All the compounds have low or moderate solubilities in alcohols or acetonitrile and are significantly more soluble in DMF or DMSO.

The complexes were prepared under normal atmospheric conditions and the nickel compounds appear to be quite stable to oxidation. The manganese complexes can be stored unchanged in a dessicator, but undergo gradual change from golden yellow to brown–yellow when exposed to the atmosphere. In solution, the manganese complexes rapidly become dark brown when exposed to atmospheric oxygen. Such a colour change commonly accompanies oxidation of Mn(II) to Mn(III), however the products of this oxidation have not yet been isolated and characterised.

Infrared Spectra

The main features of the IR spectra of the complexes are shown in Table 1. Formation of the macrocycle is confirmed by the absence of carbonyl or amine stretches from the reactants and presence of a sharp, strong band in the region 1620–1635 cm^{-1} due to the imine stretch.

In complexes **2**–**4** and **6**, a relatively sharp and intense band at 3390–3450 cm^{-1} is assigned to the ν(OH) stretch of the uncoordinated ligand alcohol groups. In the other complexes this signal is broadened by the addition of mixed stretches of coordinated or uncoordinated water or alcohol solved molecules.

The spectra of the halide complexes **1**, **2**, **7** and **8** are identical except in the 3200–3500 cm^{-1} region, the remaining complexes can be distinguished by the signals due to the anions. Signals due to the NO_3^- group in **3** and **9** are somewhat confused by overlapping ligand absorptions, but the number and intensity of bands in the 1300–1500 cm^{-1} region

TABLE 1. Physical properties of the complexes

Complex	No.	Colour	μ_{eff} (BM)		Electronic spectra in DMF (nm (l mol^{-1} cm^{-1}))	Infrared spectra; selected bands (cm^{-1})	
			300 K	93 K		ν(OH)	ν(C=N)
$[Mn_2(H_2L1)Cl_2]\cdot H_2O$	1	yellow–orange	5.83	5.87	371.2 (10,000), 264.7 (38,500) 254.5 (14,500)	3425(s)	1620(vs)
$[Mn_2(H_2L1)Br_2]$	2	yellow–orange	5.94	5.96	372.4 (17,000), 267.1 (44.000), 249.7 (12,000)	3430(s)	1620(vs)
$[Mn_2(H_2L1)(NO_3)_2]$	3	yellow–gold	5.96	6.01	373.6 (10,500), 264.9 (40,500)	3450(s)	1620(vs), 1445(s), 1380(vs)
$[Mn_2(H_2L1)(NCS)_2]$	4	yellow–gold	6.07	6.14	374.7 (12,000), 269.9 (42.500), 255.5 (15,000)	3400(m)	1620(vs), 2065(vs)
$[Mn_2(H_2L1)(CH_3COO)_2]\cdot 2CH_3OH$	5	yellow–gold	5.92	5.96	374.2 (16,000), 256.6 (64,000),[a] 372.9, 365.1, 250.0[b,c]	3410(m) 3215(m)	1625(vs), 1550(s)
$[Mn_2(H_2L1)(N_3)_2]$	6	yellow–gold	5.83	5.87	376.3, 270.6[b]	3390(m)	1620(vs), 2050(vs)
$[Ni_2(H_2L1)(H_2O)_2Cl_2]\cdot 2H_2O$	7	green–brown	2.84	2.14	590 (20), 383.8 (18,000), 267.7 (39,000), 251.5 (10,500)	3350(bs)	1630(vs)
$[Ni_2(H_2L1)(H_2O)_2Br_2]$	8	green–yellow	2.82	2.16	580 (35), 389.2 (14,500), 267.1 (32,500), 251.5 (11,500)	3350(m) 3250(sh)	1635(vs)
$[Ni_2(H_2L1)(H_2O)_2(NO_3)_2\cdot H_2O$	9	green	2.75	2.07	570.9 (22), 379.6 (13,500), 266.5 (31,000), 252.7 (11,000)	3350(bm)	1625(vs), 1440(sh), 1375(vs)
$[Ni_2(H_2L1)(NCS)_2C_2H_5OH]$	10	green–brown	2.78	2.08	584.2 (26), 379.4 (17,000), 267.7 (36,500)	3375(m)	1630(vs), 2100(s), 2050(s)
$[Ni_2(H_2L1)(CH_3COO)_2]\cdot H_2O$	11	green–yellow	2.95	2.80	587.0 (40), 386.2 (12,500) 265.3 (31,500), 252.7 (12,500)	3350(bs)	1630(vs), 1550(vs)

[a] In methanol. [b] Qualitative spectrum only. [c] In 1:1 DMF:methanol.

strongly suggest that the NO_3^- anions are coordinated. In **6** a strong band at 2050 cm^{-1} is due to the asymmetric stretch of the azide group and implies that the ligand is terminally bound (or possibly bridging via a single nitrogen atom). The asymmetric stretch of the thiocyanate group in complex **4** appears at 2065 cm^{-1}, consistent with a terminal N-bonded NCS^-. In **10** there are two bands, the weaker at 2100 cm^{-1} and a more intense signal at 2050 cm^{-1}.

The acetate complexes **5** and **11** have very similar infrared spectra, the only differences being those expected for the different solvent molecules present. Bands due to the acetate group appear as broad, strong signals at 1550 cm^{-1}, overlapping with the ligand phenyl ring vibrations. This is consistent with bidentate coordination at these groups.

Electronic Spectra

The manganese complexes show no d–d spectra, consistent with the magnetic data which imply the presence of high-spin d^5 metal ions. All of these complexes, however, exhibit three absorptions in the ultraviolet at 371–376, 264–271 and 249–256 nm. The latter two absorptions appear at almost identical positions in the uncomplexed ligand cation [13] and are therefore assigned to intraligand transitions. The first band is ascribed to a charge transfer transition and occurs in the same region for the analogous Ni(II), Cu(II), Co(II), Pb(II) and Zn(II) complexes.

The electronic spectra of the nickel(II) complexes can be interpreted in terms of approximately octahedral stereochemistry. A weak band at 570–590 nm (ϵ = 20–40 l mol^{-1} cm^{-1}) in DMF solution is assigned to the $^3A_{1g} \rightarrow {}^3T_{1g}(F)$ transition. The low energy $^3A_{1g} \rightarrow {}^3T_{2g}$ transition (generally at *c.* 1000 nm) was not observed due to the range ilimitations of the instrument used (200–900 cm^{-1}). A high intensity absorption at 379–390 nm (ϵ = 12 600–18 000 l mol^{-1} cm^{-1}) in all five nickel(II) complexes is attributed to a combination of the $^3A_{1g}$ and $^3T_{1g}(P)$ transition and a charge transfer process. The pseudo-octahedral geometry of **6** in the solid state has been established from X-ray crystallography. The electronic spectra confirm that all the nickel complexes are also six coordinate in DMF solution. The electrochemical results (see below) show that the anions dissociate in solution. Consequently, the visible spectra probably represent equilibria in which the coordinating anions are exchanging with DMF solvent molecules.

Magnetic Susceptibility

Magnetic susceptibility data were recorded in the range 93–298 K for all the complexes; the results are listed in Table 1. The room temperature moments for complexes **2**–**5** fall in the range expected for a high spin d^5 ion. In complexes **1** and **6** the moments are slightly low (5.83 μ_B per Mn). This could be attributed to the presence of a diamagnetic impurity or to some antiferromagnetic coupling. The effective moment increases slightly with decreasing temperature, suggesting that there may be a weak intramolecular ferromagnetic interaction. Similar interactions have been reported in analogous complexes and ascribed to coupling via the phenoxy bridges [9, 12].

The nickel complexes **7**–**10** exhibit room temperature moments in the range 2.75–2.82 μ_B per Ni, which are somewhat reduced from the value expected for two unpaired electrons in a six-coordinate environment. The values decrease appreciably with temperature and lie in the range 2.06–2.16 μ_B per Ni at 93 K. This can be attibuted to antiferromagnetic coupling between the Ni(II) ions in each binuclear unit. For a binuclear nickel(II) complex the data can be fitted to the equation [16]

$$\chi_M = \frac{Ng^2\beta^2}{kT} = \left[\frac{10 + 2\exp(-4J/kT)}{5 + 3\exp(-4J/kT) + \exp(-6J/kT)}\right] + N\alpha$$

Best fits of the data to this expression gave coupling constants in the range $J = -23$ to $J = -27$ cm^{-1}. The temperature-independent paramagnetism was 300–400 × 10^{-6} cgsu/mol. Similar results have been reported by Hendrickson [15]. In the complex $[Ni_2(H_2L1)(CH_3COO)_2]\cdot 2H_2O$ (**11**) coupling is much weaker ($J = -3$ cm^{-1}).

EPR

The EPR spectrum of **5** at 110 K at 1:2 methanol:DMF was recorded. The observed signal is probably not due to the $[Mn(II)]_2$ dimer, but rather to a partially oxidised Mn(II)Mn(III) species. The main feature consists of a Mn(II) six-line hyperfine spectrum centred at $g = 2.0$ with a spacing of 90 G, with ten weaker lines interspersed between them. Similar spectra have been observed for mixed valence Mn(II)Mn(III) complexes of related ligands [8], where the weak lines are ascribed to forbidden $\Delta M_I = 1$ transitions. Magnetically coupled $[Mn(II)]_2$ systems generally do not exhibit hyperfine lines.

Description of the Structures

Single crystal X-ray structure determinations have been carried out for complexes **5** and **7** as described in 'Experimental'. Perspective views of the complexes are shown in Figs. 1 and 2 and the non-hydrogen atom coordinates are listed in Table 2; selected bond lengths and angles are given in Table 3. In both cases the saturated section of the macrocycle showed some disorder. This has been modelled and the occupancies refined to 64:36 for positions C9a, C9c; C10a, C10c; C11a, C11c and O2a, O2c in **5** and

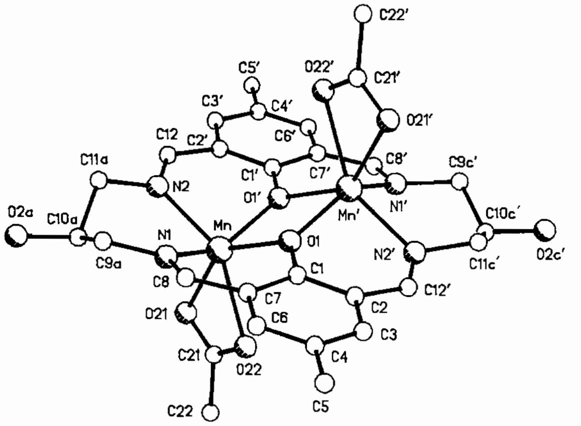

Fig. 1. Perspective view of $[Mn_2(H_2L1)(CH_3COO)_2]\cdot 2CH_3OH$ (5); the methanol solvate molecules have been omitted. Both the disordered conformations of the saturated section of the macrocycle are shown, one of each half of the centrosymmetric molecule.

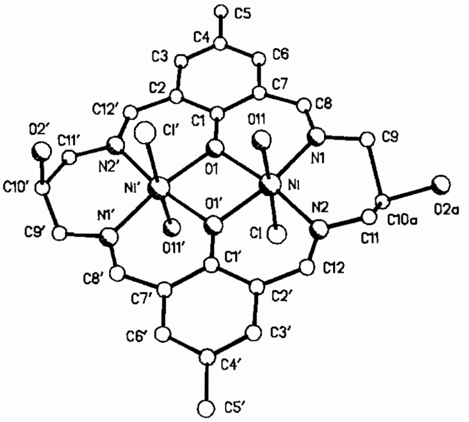

Fig. 2. Perspective view of $[Ni_2(H_2L1)(H_2O)_2Cl_2]\cdot 2H_2O$ (7) with the solvate water molecules omitted. Both conformations of the disordered alcohol group are shown, one on each half of the centrosymmetric molecule.

60:40 for the atom pairs C10, O2 and C10a, O10a in 7.

The manganese complex 5 is centrosymmetric, each manganese atom is coordinated to two imine nitrogen donors and two bridging phenolate groups from the macrocycle. The coordination sphere is completed by a bidentate acetate ligand. The metal atoms are therefore six coordinate but their irregular geometry may be best described as square pyramidal, with the acetate group as axial ligand. The manganese atoms are 0.77 Å on either side of the mean plane of the macrocyclic donors (O1, O1′, N1, N1′, N2 and N2′) and the Mn–Mn′ distance is 3.34 Å. The structure of 7 is also centrosymmetric and each nickel atom is coordinated to two imine nitrogen atoms and two bridging phenoxide donors. In contrast to 5, however, the nickel atoms have quite regular octahedral geometry. The axial ligands are one chloride ion and one water molecule and the nickel atoms are within 0.025 Å of the mean plane of the macrocyclic donor with a Ni–Ni′ separation of 3.10 Å. Both structures contain solvate molecules

TABLE 2. Atomic coordinates ($\times 10^4$)

Atom	x	y	z
$[Mn_2(H_2L1)(CH_3COO)_2]\cdot 2CH_3OH$			
Mn	284(1)	1699(1)	3614(1)
O(1)	1191(2)	123(2)	5412(2)
C(1)	2168(3)	438(3)	5926(3)
C(2)	1956(4)	−205(3)	7489(3)
C(3)	3071(4)	82(3)	7984(4)
C(4)	4430(4)	950(3)	7013(4)
C(5)	5668(4)	1181(4)	7560(4)
C(6)	4589(4)	1610(3)	5505(4)
C(7)	3471(4)	1414(3)	4947(3)
C(8)	3793(4)	2222(3)	3338(3)
N(1)	2866(3)	2385(3)	2584(3)
C(9a)	3708(5)	3129(5)	969(5)
C(9c)	3221(11)	3580(11)	957(10)
C(10a)	2452(6)	3760(5)	110(5)
C(10c)	2971(13)	3141(12)	−108(11)
O(2a)	3372(4)	4716(4)	−1355(4)
O(2c)	3770(8)	4195(8)	−1594(7)
C(11a)	1771(6)	2511(5)	52(5)
C(11c)	1318(11)	2965(10)	−12(9)
N(2)	445(3)	1727(3)	1467(3)
C(12)	−594(4)	1129(3)	1332(3)
O(21)	−1480(3)	3736(3)	3081(3)
O(22)	−640(3)	3038(3)	5000(3)
C(21)	−1466(4)	3928(3)	4177(3)
C(22)	−2448(4)	5204(4)	4484(4)
O(41)	8820(4)	2347(3)	8024(3)
C(41)	7958(5)	3571(4)	8233(4)
$[Ni_2(H_2L1)(H_2O)_2Cl_2]\cdot 2H_2O$			
Ni	2074(1)	3941(1)	8302(1)
O(1)	1292(2)	3425(2)	8619(6)
C(1)	902(3)	3533(3)	8764(7)
C(2)	357(3)	3104(3)	8864(7)
C(3)	−51(3)	3241(4)	9011(7)
C(4)	39(4)	3747(4)	9053(7)
C(5)	−423(4)	3850(4)	9144(9)
C(6)	567(3)	4155(3)	8949(7)
C(7)	993(4)	4064(3)	8825(8)
C(8)	1509(4)	4532(4)	8750(10)
N(1)	1972(3)	4573(3)	8642(8)
C(9)	2434(5)	5106(4)	8718(16)
C(10a)	2823(13)	5168(12)	7256(33)
C(10)	2900(6)	5220(6)	8025(16)
O(2)	2714(5)	5113(5)	6388(14)
O(2a)	3288(15)	5791(16)	7926(42)
C(11)	3169(4)	4896(5)	8189(16)
N(2)	2875(3)	4349(3)	7992(8)
C(12)	3148(3)	4124(3)	7830(8)
Cl	1913(1)	3983(1)	5784(3)
O(11)	2235(3)	3876(3)	10465(7)
O(20)	2345(7)	4559(7)	12606(17)
O(30)	994(8)	460(8)	5934(22)

TABLE 3. Selected bond lengths (Å) and angles (°)

$[Mn_2(H_2L1)(CH_3COO)_2]\cdot 2CH_3OH$			
Mn–O(1)	2.149(2)	Mn–N(1)	2.201(3)
Mn–N(2)	2.217(3)	Mn–O(21)	2.290(2)
Mn–O(22)	2.281(3)	Mn–O(1′)	2.108(2)
O(1)–Mn–N(1)	82.4(1)	O(1)–Mn–N(2)	131.8(1)
N(1)–Mn–N(2)	88.7(1)	O(1)–Mn–O(21)	140.5(1)
N(1)–Mn–O(21)	109.5(1)	N(2)–Mn–O(21)	87.0(1)
O(1)–Mn–O(22)	85.0(1)	N(1)–Mn–O(22)	96.3(1)
N(2)–Mn–O(22)	143.2(1)	O(21)–Mn–O(22)	56.9(1)
O(1)–Mn–O(1′)	76.4(1)	N(1)–Mn–O(1′)	143.4(1)
N(2)–Mn–O(1′)	83.9(1)	O(21)–Mn–O(1′)	105.8(1)
O(22)–Mn–O(1′)	110.9(1)	Mn–O(1)–Mn′	103.6(1)
$[Ni_2(H_2L1)(H_2O)_2Cl_2]\cdot 2H_2O$			
Ni–O(1)	2.014(5)	Ni–N(1)	2.016(9)
Ni–N(2)	2.026(6)	Ni–Cl	2.521(3)
Ni–O(11)	2.195(8)	Ni–O(1′)	1.992(7)
O(1)–Ni–N(1)	91.5(3)	O(1)–Ni–N(2)	170.2(3)
N(1)–Ni–N(2)	98.0(3)	O(1)–Ni–Cl	91.2(2)
N(1)–Ni–Cl	90.2(2)	N(2)–Ni–Cl	90.6(2)
O(1)–Ni–O(11)	89.7(2)	N(1)–Ni–O(11)	92.9(3)
N(2)–Ni–O(11)	88.0(3)	Cl–Ni–O(11)	176.7(3)
O(1)–Ni–O(1′)	78.5(3)	N(1)–Ni–O(1′)	170.1(3)
N(2)–Ni–O(1′)	91.8(3)	Cl–Ni–O(1′)	90.6(2)
O(11)–Ni–O(1′)	86.5(3)	Ni–O(1)–Ni′	101.5(3)

which do not exhibit any significant interactions with the complex molecules.

The differences between the two structures are due to a combination of stereochemical preference and ionic size. The smaller nickel(II) ion (radius 0.83 Å) can be accommodated within the plane of the macrocycle and exhibits its preferred octahedral coordination. High-spin manganese(II) has no stereochemical preferences and its larger radius (0.97 Å) means that it is less easily accommodated in the macrocyclic plane. As expected, the mean Mn(II) to phenoxy or imine bonds (2.13 and 2.21 Å) are typical for Mn(II) and significantly longer than the equivalent bonds in the Ni(II) case (2.00 and 2.02 Å). Comparison of the physical data for the two series of compounds suggests that the structures of **5** and **7** are typical of the manganese and nickel complexes, respectively.

Elelectrochemistry

A preliminary study of the electrochemical behaviour in DMF of complexes **1**–**3** and **7**–**11** was made using cyclic voltammetry; complex **5** was examined in 1:1 DMF/methanol. Figures 3 and 4 show representative cyclic voltammograms. All cyclic voltammograms were recorded at 100 mV s^{-1} and potentials are versus SCE.

Manganese complexes 1–3, 5

The electrochemical responses of complexes **1**–**3** show common features suggesting that the monodentate anionic ligands dissociate in the DMF electrolyte. Figure 3(a) shows the cyclic voltammogram of complex **3**. For each complex there is a broad oxidation peak at $E_{pa} \simeq 0.32$ V and two coupled reduction peaks at $E_{pc} \simeq 0.06$ and -0.07 V. We assume that a metal-based oxidation occurs in this process with the following chemical steps leading to two reduction peaks. Two closely-spaced irreversible reduction processes occur at $E_{pc} \simeq -1.81$ and -1.93 V and a further irreversible reduction process is seen at $E_{pc} \simeq -2.15$ V. In addition, for complex **1** there is an irreversible oxidation process at $E_{pa} \simeq$ 0.90 V due to Cl^- oxidation and for complex **2** an irreversible oxidation at $E_{pa} \simeq 0.55$ V due to Br^- oxidation.

The electrochemistry of complex **5** was studied in a 1:1 DMF:methanol electrolyte. As shown in Fig. 3(b), complex **5** exhibits a chemically reversible oxidation step at $E^{\circ\prime} = 0.11$ V ($\Delta E_p = 120$ mV) and two further very broad oxidation peaks at $E_{pa} \simeq 0.73$ and 0.95 V. We assign the reversible oxidation process to formation of the mixed valence dimer Mn(II)Mn(III). Two broad irreversible reduction peaks are seen at $E_{pc} \simeq -1.86$ and -2.10 V.

Nickel complexes 7–11

As is found for the manganese complexes **1**–**3**, the electrochemical behaviour of complexes **7**–**10** show some common features consistent with the dissociation of the monodentate anionic ligands.

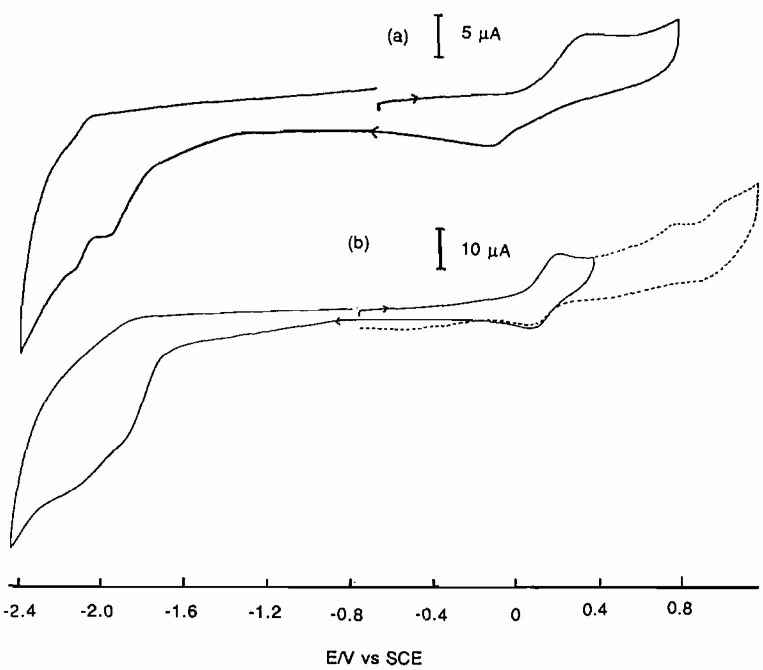

Fig. 3. Cyclic voltammograms at 100 mV s^{-1}; (a) complex 3, 1 mM in DMF/0.1 M TEAP; (b) complex 5, 1 mM in 1:1 DMF: methanol/0.1 M TEAP.

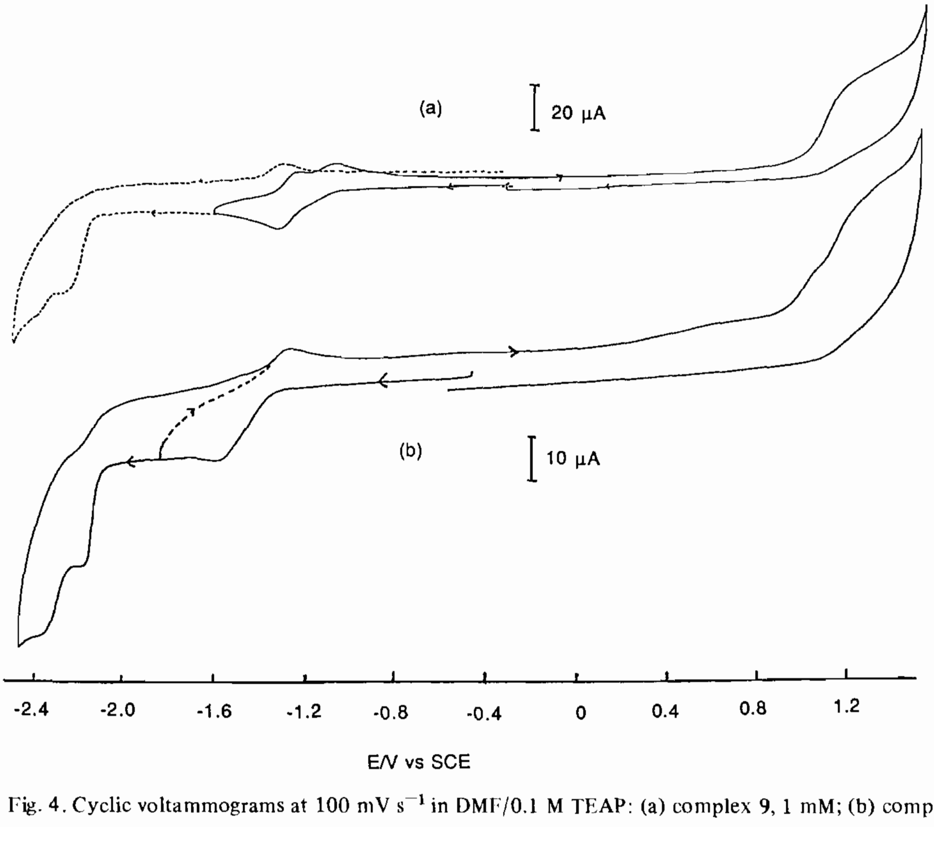

Fig. 4. Cyclic voltammograms at 100 mV s^{-1} in DMF/0.1 M TEAP: (a) complex 9, 1 mM; (b) complex 11, 1 mM.

In Fig. 4(a) is shown the cyclic voltammogram of complex **9**. All complexes **7**–**10** exhibit two closely-spaced reduction steps; the cathodic components of the waves merge giving a single peak at E_{pc} = –1.32 V and associated oxidation peaks appear at E_{pa} = –1.23 and –1.06 V. The cyclic voltammogram of complex **11** given in Fig. 4(b) shows that for this complex, the reduction is shifted to more negative potentials; E_{pc} = –1.64 V and there is a single anodic component at E_{pa} = –1.32 V. These processes may reasonably be assigned to metal-based reductions. All complexes undergo two further irreversible reduction steps at $E_{pc} \simeq -2.15$ and –2.35 V and an irreversible oxidation at $E_{pa} \simeq 1.2$ V. Complex **11** has an additional irreversible oxidation at $E_{pa} \simeq$ 1.0 V and complexes 7, **8** and **10** exhibit additional irreversible oxidation processes corresponding to oxidation of Cl^- at $E_{pa} \simeq 0.90$ V, Br^- at $E_{pa} \simeq 0.55$ V and SCN^- at $E_{pa} \simeq 0.60$ and 1.1 V, respectively.

Conclusions

In the complexes under investigation, the Schiff base macrocycle (H_4L1), potentially an octadentate ligand, utilises only six donors for ligation to Mn(II) and Ni(II) ions. Two endogenous phenoxy bridges are formed between adjacent metal ions in discrete binuclear units. The two alcoholic functions of the macrocycle remain protonated and do not participate in ligation with metal ions. This behaviour contrasts with their involvement in coordination with Pb(II) ions [13] in the analogous Pb(II) complex $[Pb_2(H_2L1)](ClO_4)_2$. This difference may be attributed to the difference in the nature of the metal ions and the mismatch between the size of the metal ions and the ligand cavity. The manganese(II) complexes with Cl^-, Br^-, NO_3^- and NCS^- counter ions are five coordinate having approximately square pyramidal geometry around each manganese(II) ion. The four positions in the basal plane are occupied by the N_2O_2 donor set of the macrocyclic ligand and the fifth axial position is occupied by the anion. In $[Mn_2(H_2L1)(MeCO_2)_2]\cdot MeOH$ the metal is six coordinate with the acetate groups acting as bidentate ligands.

All the nickel(II) complexes are six coordinate, having octahedral or distorted octahedral geometry around each metal ion. Again, four positions in the ligand plane are occupied by the N_2O_2 donor set of the macrocycle and the two axial positions are occupied by anions and/or water molecules.

Efforts are being made to isolate binuclear, tetranuclear [11, 17] and polynuclear [18] complexes having metal ions in different oxidation states. In these complexes, macrocyclic ligands may provide endogenous alkoxy and phenoxy bridges on deprotonation and may hold four or more metal ions by intramolecular or intermolecular bridges.

Supplementary Material

Tables of bond lengths, bond angles, anisotropic thermal parameters, hydrogen atom parameters and structure factors are available from the authors on request.

Acknowledgements

We thank the New Zealand University Grants Committee for the award of a postdoctoral fellowship to S.S.T. and the Punjabi University, Patiala, India, for granting him leave. We are grateful to Dr E. Ainscough for obtaining EPR spectra.

References

1 V. L. Pecoraro, *Photochem. Photobiol., 48* (1988) 249.

2 R. M. Fronko, J. E. Penner-Hahn and C. J. Bender, *J. Am. Chem. Soc., 110* (1988) 7554.

3 J. R. Lancaster (ed.), *The Bioinorganic Chemistry of Nickel*, VCH, New York, 1988.

4 R. A. Scott, S. A. Wallin, M. Czechowski, D. V. Der-Vartanian, J. LeGall, H. D. Peck and I. Moura, *J. Am. Chem. Soc., 106* (1984) 6864.

5 R. M. Buchanan, M. S. Mashuta, K. J. Oberhausen, J. F. Richardson, Q. Li and D. N. Hendrickson, *J. Am. Chem. Soc., 111* (1989) 4497.

6 K. Wieghardt, U. Bossek, B. Nuber, J. Weiss, J. Bonvoisin, M. Corbella, S. E. Vitols and J. J. Girerd, *J. Am. Chem. Soc., 110* (1988) 7398.

7 D. K. Towle, C. A. Botsford and D. J. Hodgson, *Inorg. Chim. Acta, 141* (1988) 167.

8 J. S. Bashkin, A. R. Schake, J. B. Vincent, H.-R. Chang, Q. Li, J. C. Hoffman, G. Christou and D. N. Hendrickson, *J. Chem. Soc., Chem. Commun.*, (1988) 700.

9 H.-R. Chang, S. K. Larsen, P. D. W. Boyd, C. G. Pierpont and D. N. Hendrickson, *J. Am. Chem. Soc., 110* (1988) 4565.

10 S. Raghunathan, C. Stevenson, J. Nelson and V. McKee, *J. Chem. Soc., Chem. Commun.*, (1989) 5.

11 V. McKee and S. S. Tandon, *J. Chem. Soc., Chem. Commun.*, (1988) 1334.

12 D. Luneau, J.-M. Savariault, P. Cassoux and J.-P. Tuchagues, *J. Chem. Soc., Dalton Trans.*, (1988) 1225.

13 S. S. Tandon and V. McKee, *J. Chem. Soc., Dalton Trans.*, (1989) 19.

14 G. M. Sheldrick, *SHELXTL User Manual, Revision 4.1*, Nicolet XRD Corporation, Madison, WI, 1984.

15 G. L. Spiro, S. L. Lambert, T. J. Smith, E. N. Duesler, R. R. Gagne and D. N. Hendrickson, *Inorg. Chem., 20* (1981) 1229.

16 R. L. Carlin, *Magnetochemistry*, Springer, Berlin, 1986.

17 V. McKee and S. S. Tandon, *J. Chem. Soc., Chem. Commun.*, (1988) 385.

18 V. McKee and S. S. Tandon, *Inorg. Chem., 28* (1989) 2901.